Available online at www.sciencedirect.com

ScienceDirect

Ceramics International 35 (2009) 1447–1452

CERAMICS
INTERNATIONAL

www.elsevier.com/locate/ceramint

Synthesis and characterization of diopside glass–ceramic matrix composite reinforced with aluminum titanate

M. Yousefi [a], P. Alizadeh [b,*], B. Eftekhari Yekta [c], F. Molaie [d], N. Ghafoorian [d], M. Montazerian [b]

[a] *Islamic Azad University, Shahr-e-Rey Branch, Shahr-e-Rey, Iran*
[b] *School of Engineering, Tarbiat Modares University, Tehran, Iran*
[c] *Ceramic Division, Department of Materials, Iran University of Science and Technology, Tehran, Iran*
[d] *Department of Chemistry, Sharif University of Technology, Tehran, Iran*

Received 12 October 2007; received in revised form 8 July 2008; accepted 25 July 2008
Available online 14 August 2008

Abstract

Glass–ceramic composites in the SiO_2–CaO–MgO–(Na_2O) system, reinforced with 5, 10 and 20 wt.% aluminum titanate were synthesized by pressureless sintering. Optimum sintering temperatures with maximum relative density were determined for each composition. The composites were fired above the crystallization peak temperature of glass–ceramic. Mechanical properties of glass–ceramic and sintered composites, such as fracture toughness, flexural strength and Vickers microhardness, were investigated. The sintered composites were characterized by scanning electron microscopy (SEM), energy dispersion spectroscopy (EDS) and X-ray diffraction (XRD). The results showed that the composite containing 10 wt.% aluminum titanate has desirable behavior in comparison to the base glass–ceramic and the other compositions. It seems that crack deflection by aluminum titanate particles is the prevalent mechanism for improving mechanical characteristics.

Keywords: A. Sintering; B. Composites; D. Al_2TiO_5; D. Glass–ceramics

1. Introduction

Owing to their favorable properties, i.e. low density, low cost and tailor-made thermal and mechanical properties, the glass–ceramics are a category of important engineering materials. But for the improvement of the mechanical properties, e.g. flexural strength, microhardness and toughness, the use of composite materials has been considered. Such a composite can be fabricated by incorporating in the glass–ceramic matrix a second constituent in the form of long or chopped fibers, whiskers, platelets or particles [1].

Aluminum titanate (Al_2TiO_5: AT) owing to the fact that it has low thermal expansion, high thermal shock resistance and high melting point, these properties make it as an interesting ceramic material [2]. The use of this material as a reinforcing material in mullite–AT composites and alumina–AT composites were reported for improving thermal shock resistance and mechanical properties [3–6]. Also, it is said that in the AT–glass matrix composite, aluminum titanate has improved the thermal shock resistance of the matrix [7]. Additionally, among different kinds of ceramic and metallic particles that can be used as a reinforcing phase in glass–ceramic composites, there is no report on using AT to improve the property of these materials.

The sinterability and mechanical properties of glass–ceramic in the SiO_2–MgO–CaO–(Na_2O) system has been investigated previously. Previous study showed that by using some additives such as Fe_2O_3 and Cr_2O_3, pressureless sintering process can be used to produce glass–ceramics in this system with desirable mechanical properties and appropriate final density [8]. Optimum composition obtained from sintering method was selected as a matrix of composite in this study.

For improvement of mechanical properties, the sintering behavior and mechanical properties of glass–ceramic by incorporating aluminum titanate in the form of particles has been studied. The properties of composites were compared with the base glass–ceramic and the optimum composition and sintering condition were determined.

---

* Corresponding author at: School of Engineering, Tarbiat Modares University, P.O. Box: 14115-143, Tehran, Iran.
E-mail address: p-alizadeh@modares.ac.ir (P. Alizadeh).

0272-8842/$34.00 © 2008 Elsevier Ltd and Techna Group S.r.l. All rights reserved.
doi:10.1016/j.ceramint.2008.07.020

2. Experimental procedure

The composition of glass (wt.%) is 59.68 SiO_2, 12.23 CaO, 15.02 MgO, 5.08 Na_2O, 4.00 Fe_2O_3 and 4.00 Cr_2O_3. The sinterability of this glass was previously investigated [8]. All of the materials used for the preparation of the glass were reagent grade. The weighed batch material, after mixing was melted in a platinum crucible in an electric furnace at 1400 °C for 1 h. The melt was then quenched in the distilled water to obtain a frit. The frit was immediately dried at 120 °C for 2 h.

The frit was ground in an electric agate mortar (Fritsch, Pulverisette 2) for 1 h and then fast-milled for 40 min in ethanol media. The particle size measurement of the powder glass, which was carried out by a laser particle size analyzer (Fritsch, Analysette 22) showed a mean particle size of about 7 μm. The composite powder mixture was prepared by adding 5, 10 and 20 wt.% aluminum titanate powder (Aldrich, mean particle size 26 μm) to the glass powder and named as A, B and C, respectively. The mixtures were homogenized by dispersing them in acetone by hand mixing and ultrasonic vibration for 2 min. Drying was carried out by simultaneous mixing and heating the suspension. The dried, homogenous powder mixture was pressed into discs (12 mm in diameter and 2 mm thickness) using a laboratory uniaxial hydraulic press at final pressure of 65 MPa. Methyl cellulose (0.45 wt.%) was used as a binder.

Sintering was carried out in an electric furnace at 940–1150 °C at a heating rate of 10 °C min^{-1}. The soaking time was 3 h. The crystallized samples were then subjected to XRD analysis using a powder diffractometer (Siemens D-500, Cu Kα radiation at 40 kV). Silicon powder was used as the standard. Microstructural studies on the samples were done by scanning electron microscopy (SEM; Cambridge, Stereo scan 360). The bulk and powder densities of sintered samples were determined by Archimedes method and gas pycnometery (Micromeritics, Accupyc 1330). The flexural strength and the fracture toughness of the glass–ceramic and composites were measured in air at room temperature using an Instron Universal Testing Machine-1196 machine at a crosshead speed of 0.5 and 0.05 mm/min, respectively. The flexural strength measurements were performed on bar specimens (2.5 mm × 2.5 mm × 25 mm) using a three-point bend fixture with a span of 20 mm (EN 843-1). The fracture strength measurements were performed on single edge-notched bar (SENB) specimens (2.5 mm × 5 mm × 25 mm) with a span of 20 mm and a half-thickness notch was made using a 0.3 mm thick diamond wafering blade. At least six specimens were tested for each test condition. The fracture toughness value was calculated according to ASTM E399.

A Vickers microhardness tester with a diamond pyramid indenter (Buehler, Micromet 1) was used to measure microhardness. The load was 100 g and the loading time was 30 s. Data of hardness were determined using at least 10 indentations on each polished specimen.

3. Results and discussion

Fig. 1 shows the relative density of the glass–ceramic and composites as a function of sintering temperatures after 3 h. The sintering temperatures for glass–ceramic and composites A, B and C were obtained 1000, 1030, 1060 and 1090 °C, respectively. The crystallization peak temperature of the glass phase is 858 °C [8]. Therefore sintering was done at higher temperatures than the crystallization temperature. The measured linear shrinkage percent was 16.54, 16.33, 15.58 and 13.23, for glass–ceramic and composites A, B and C, respectively. According to these results, by increasing the weight percent of aluminum titanate, the glassy phase is not enough to guarantee a pressureless viscous flow sintering process and leads to increase sintering temperature as well as reducing maximum shrinkage. The use of higher temperatures for each sample caused the occurrence of bloating effect and decreasing of shrinkage. Bloating of the specimens at higher temperatures is probably due to the reduction of Fe_2O_3 to FeO, and escape of oxygen from the body [9].

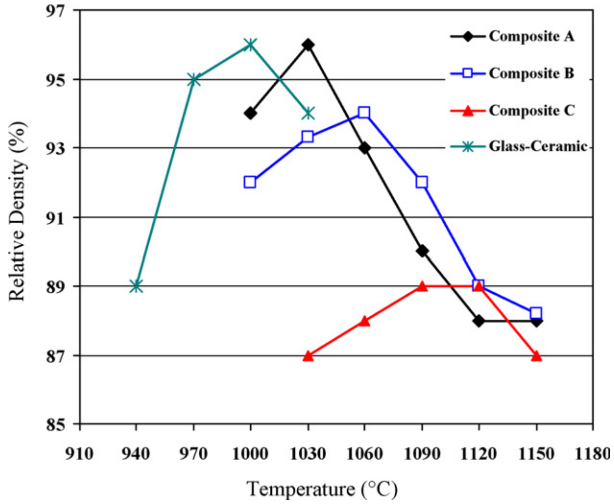

Fig. 1. Relative density of the specimens vs. sintering temperatures.

Fig. 2 shows the X-ray diffraction patterns of the glass–ceramic and the composites after sintering procedure at their final temperatures. Table 1 summarizes the existing phases in various samples. Accordingly, the diopside peak intensity of composite C decreased in comparison to other compositions. It seems that diopside is dissolved at higher temperatures. The presence of aluminum oxide and rutile in minor amounts represents decomposition of aluminum titanate in this sample.

The microstructure of the glass–ceramic and sintered composites has been shown in Fig. 3(a)–(d). The glass–ceramic mainly contains diopside crystals in the dark residual glass matrix, and brighter chromium spinel phase is also observed (Fig. 3(a)). According to the SEM images of the composites (Fig. 3(b)–(d)), increasing of weight percentage of aluminum titanate increased the volume fraction of porosity. Additionally, the bright particles with particle size of about 30 μm are aluminum titanate and brighter ones with mean particle size of about 2 μm are chromium spinel phase. A glassy phase around the AT particles is also observed.

Fig. 4 depicts a backscattered SEM micrograph of the aluminum titanate particle in composite C at higher magnification. In this figure, three distinct regions, which are labeled on the drawing, can be identified. The region A is an

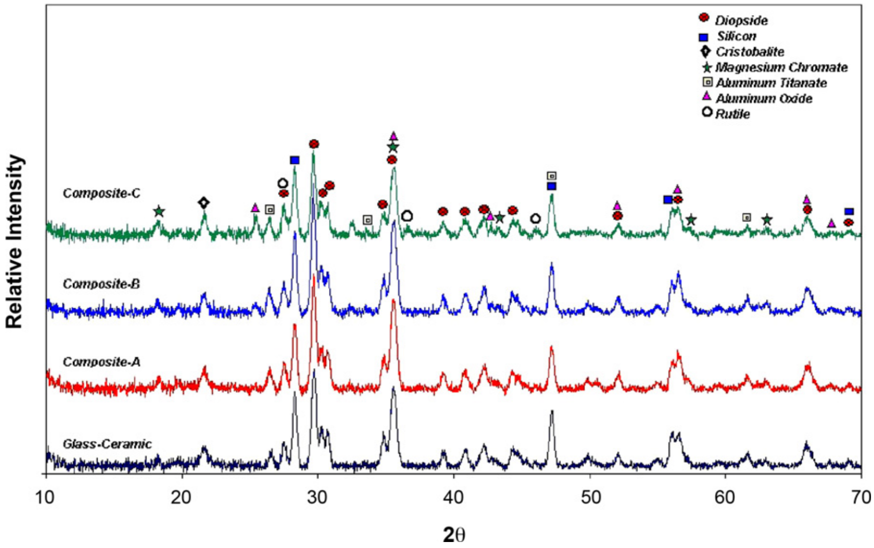

Fig. 2. XRD patterns of base glass–ceramic and composites after heat treatment at final sintering temperatures for 3 h.

aluminum titanate particle. The region B is the glassy phase around the aluminum titanate particle, which has the bright particles of chromium spinel phase within it. The region C, which is the matrix of composite, mainly contains diopside crystals (bright area) and residual glass (dark area) [8]. With attention to Fig. 4, it seems that the aluminum titanate (a duller matrix in region A) is decomposed in composite C. The EDAX analyses (Fig. 5(a) and (b)) of the light and dark areas in the particle confirmed that the former area is rich in titanium oxide and the later one is rich in aluminum oxide which was already represented in XRD patterns (Fig. 2). The EDAX analysis of the glassy phase (region B) is shown in Fig. 5(c). The presence of titanium and aluminum peaks is attributed to dissolution of aluminum titanate in the glassy phase, which could inhibit crystallization of the glass matrix by increasing its viscosity and changing the composition [10]. On the other hand, the existence of radial cracks in the glassy phase is clearly observed. These cracks can be originated from the large mismatch between the linear coefficients of thermal expansion of aluminum titanate, residual glassy phase and diopside that leads to impose thermal stresses during cooling of glass–ceramic matrix from sintering temperature. The thermal expansion coefficients of diopside and aluminum titanate are 5.0×10^{-6} and $(1.0\text{–}1.5) \times 10^{-6}\ {}^{\circ}\mathrm{C}^{-1}$ (20–600 °C), respectively [1,2].

Table 1
Crystalline phases in prepared composites

Samples	Crystalline phases
Glass–ceramic	Diopside, cristobalite[a], magnesium chromate[a]
Composite A	Diopside, cristobalite, magnesium chromate[a], aluminum titanate
Composite B	Diopside, cristobalite, magnesium chromate[a], aluminum titanate
Composite C	Diopside, cristobalite, magnesium chromate[a], aluminum titanate, rutile[a], aluminum oxide[a]

[a] Minor phases.

As it was pointed out, by increasing the content of aluminum titanate in the composites, the sintering temperatures of them increased. The increase in the sintering temperatures intensified the decomposition and dissolution of aluminum titanate. Therefore, composite containing 20 wt.% aluminum titanate showed the maximum dissolution and decomposition, which reduced the peak intensity of aluminum titanate in the XRD pattern (Fig. 2).

Mechanical characteristics of the composites and the glass–ceramic as well as their relative density at sintering temperatures have been listed in Table 2. As it is observed, with incorporating of 5 and 10 wt.% of aluminum titanate to the glass–ceramic matrix, the bending strength values and microhardness were clearly increased. The relative density of composite C is much lower than glass–ceramic; therefore its mechanical properties should not be as same as the other compositions. It seems that the presence of 20 wt.% AT in the matrix interferes with viscous flow sintering, which is essential for further densification, leads to an enhancement of the viscosity of glassy phase and an incorporation of more porosity into the matrix. Additionally, dissolution of diopside and AT in composite C at sintering temperature (1090 °C) is another reason for its poor mechanical characteristics.

A comparison between XRD patterns of composites A and B reveals that the amount of diopside phase is similar in both composites (Fig. 2). Also, the relative density of composite B is lower than composite A (Table 2). However, composite B has a better bending strength and hardness in comparison to composite A. It can be concluded that the presence of rigid AT phase in the matrix could be the responsible phenomenon for better mechanical properties of composite B. It is obvious (Table 2) that the fracture toughness values of all the composites are lower than the glass–ceramic.

In order to investigate the observed mechanical properties of the composites, the properties of aluminum titanate should be considered briefly. It is known that ceramic materials composed of highly anisotropic crystals, such as aluminum titanate and

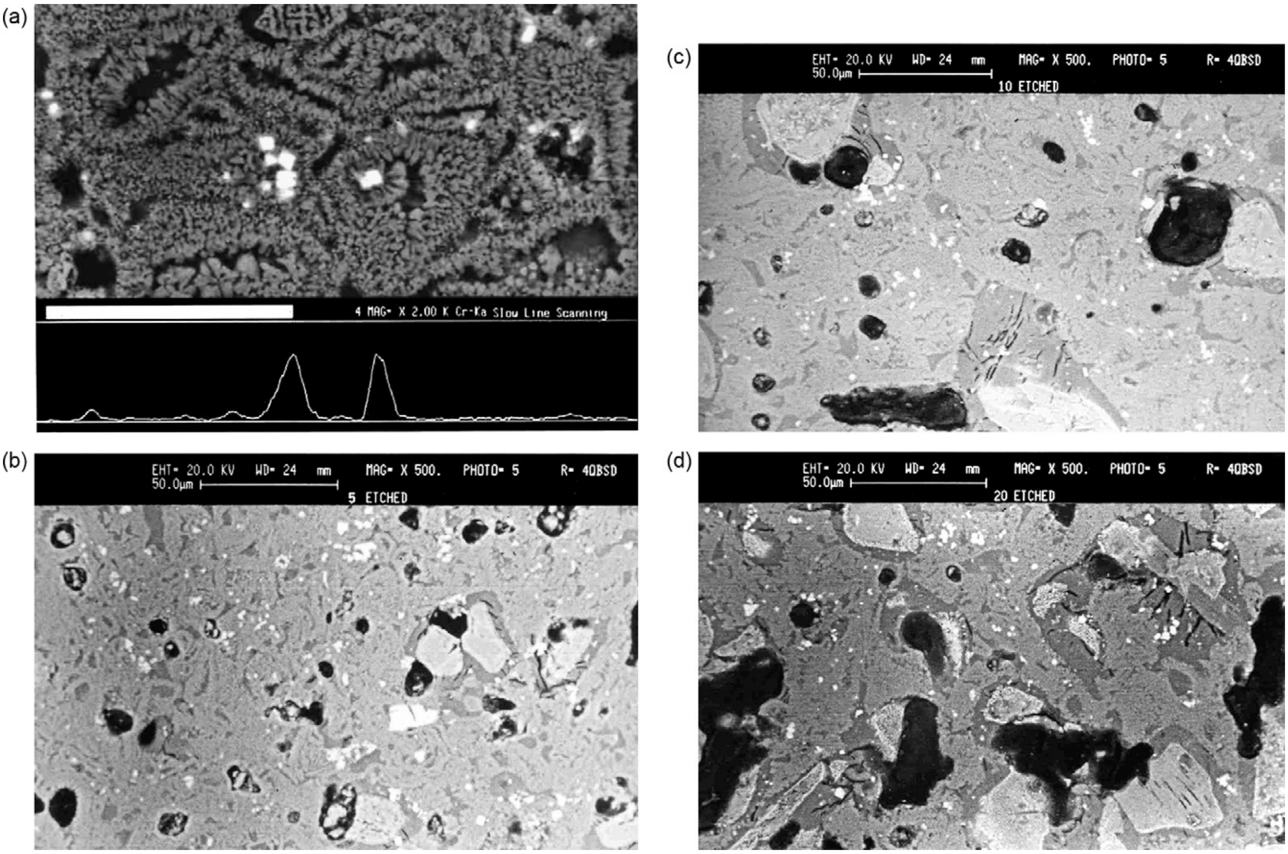

Fig. 3. SEM micrographs of the sintered samples: (a) glass–ceramic, (b) composite A, (c) composite B and (d) composite C.

other pseudobrookite-type compounds inherently contain grain boundary microcracks due to the thermal stresses generated during cooling. These cracks influence the properties of these ceramics, i.e. low mechanical strength and Young's modulus, low thermal expansion, low thermal diffusivity, and high resistance to crack propagation which is responsible for improving fracture toughness of the body. On the other hand, at high temperature, crack healing strengthens aluminum titanate bodies. It was also shown that the healing of microcracks at high temperature (1000–1110 °C) increased the mechanical strength and Young's modulus of aluminum titanate. Bending strength increased from 62 MPa at room temperature to 280 MPa at 1100 °C. Young's modulus also increased from 29 GPa at room temperature to 99 GPa at 1100 °C [11].

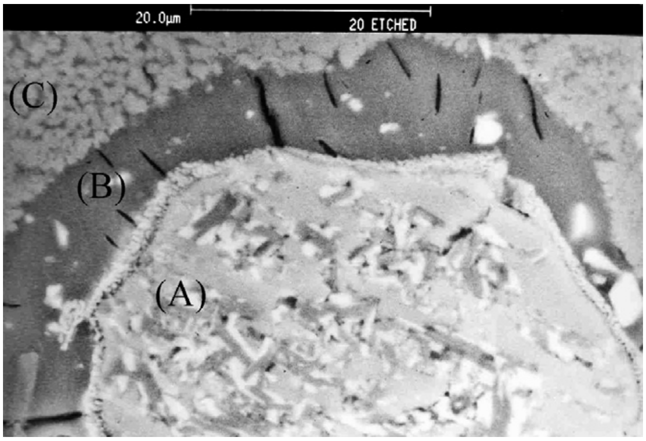

Fig. 4. SEM micrograph of aluminum titanate particle in composite C.

In the present work, the bending strength and hardness of composites A and B increase due to the presence of AT particles. This phenomenon has also been observed in the mullite–AT composite for which the bending strength of as-sintered specimens increased with increasing aluminum titanate content up to 44 vol.% and decreased at higher contents [3].

It seems that AT particles in the glass–ceramic matrix undergoes the microcrack healing due to sintering at high temperature and approximately moderate cooling rate. Also hydrostatic pressure that is exerted by matrix on AT particles facilitates the closure of microcracks. Therefore, by considering the high-temperature properties of AT due to microcrack healing, the presence of high-strength AT with high modulus of elasticity in the glass–ceramic matrix increases the bending strength and hardness of composites A and B. But fracture toughness decreases due to closure of microcracks, since microcrack formation is the prevalent mechanism of improving toughness in AT ceramics [2]. The presence of radial cracks around the AT particles (Fig. 4) and high amount of porosity are another factors that reduce the fracture toughness.

As it is mentioned, at higher temperatures (in composite C and Fig. 4) aluminum titanate with lower density (3.15 g/cm^3)

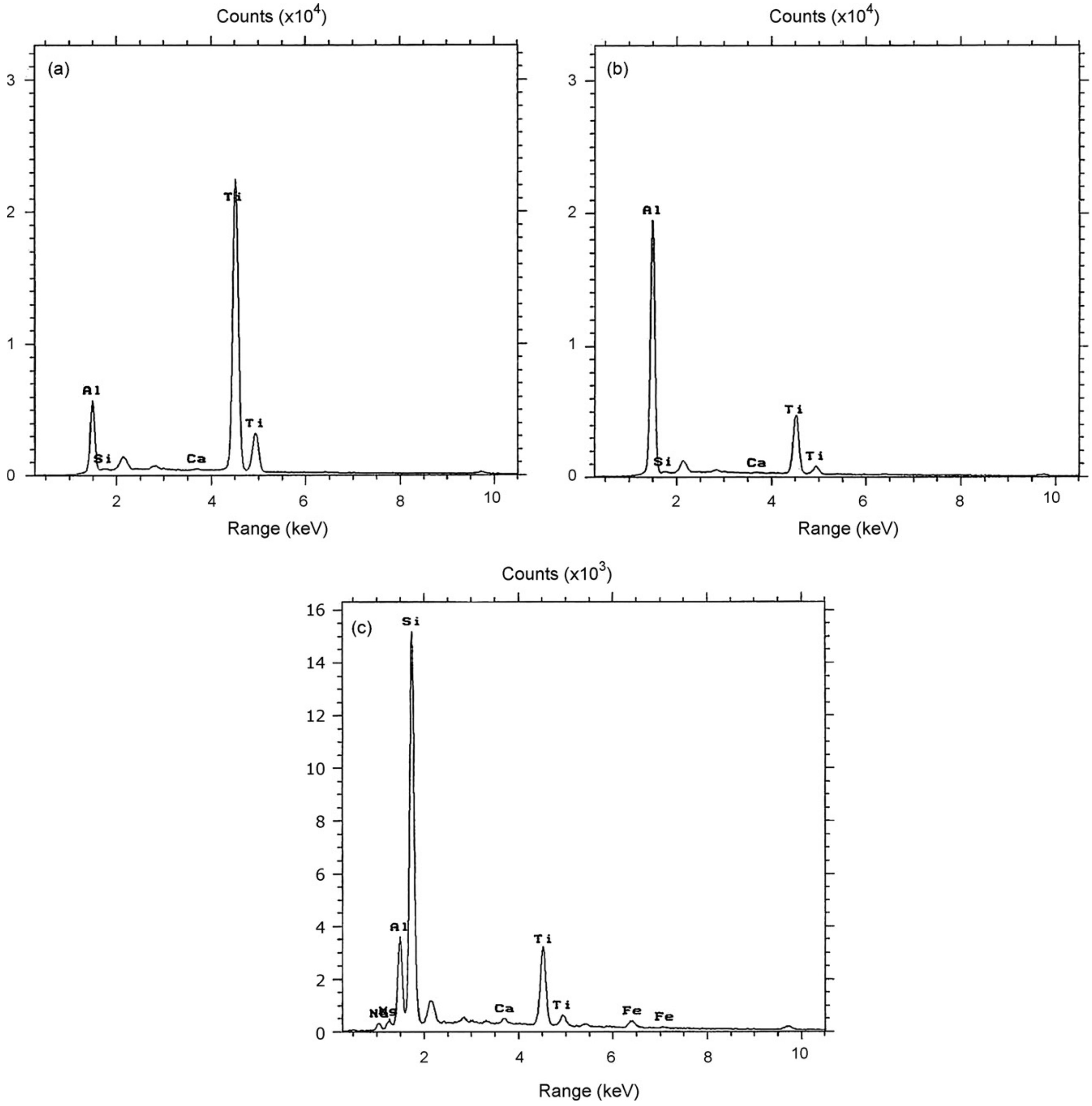

Fig. 5. EDAX analyses of (a) bright area and (b) dark area in the AT particle (c) glassy phase around the AT particle.

is decomposed to phases such as aluminum oxide and rutile with higher density (4 and 4.23 g/cm^3, respectively). This reaction can also be the cause of an increase of porosity and a decrease of fracture toughness in composite C.

A characteristic Vickers indentation crack for composite B in Fig. 6 shows crack deflection by an AT particle in the glass–ceramic matrix. Although, many microstructural factors such as particle size, shape, aspect ratio of the AT and crystallinity

Table 2
Properties of prepared composites and the glass–ceramic matrix

Samples	Bending strength (MPa)	Vickers microhardness (GPa)	Fracture toughness (MPa m$^{0.5}$)	Relative density
Glass–ceramic	82.23 ± 8.34	5.94 ± 0.52	1.48 ± 0.09	0.96
Composite A	118.30 ± 13.82	6.28 ± 0.41	1.34 ± 0.06	0.96
Composite B	120.55 ± 12.94	7.06 ± 0.81	1.30 ± 0.07	0.93
Composite C	72.43 ± 4.30	6.43 ± 1.15	1.20 ± 0.15	0.89

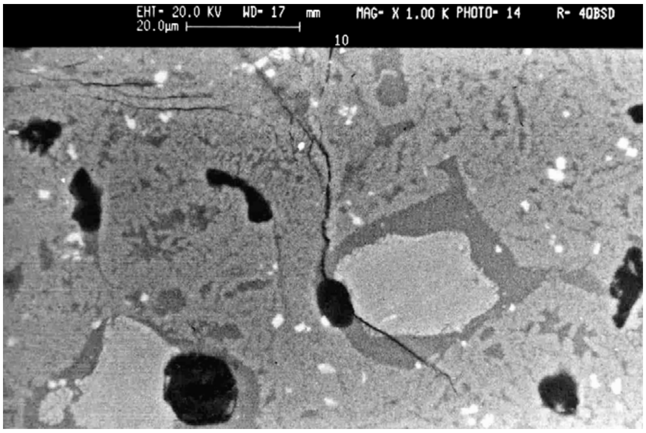

Fig. 6. SEM micrograph of crack deflection after indentation in composite B.

percentage of diopside can influence the propagation of a crack front. It seems that crack deflection can be related to large mismatch in Young's modulus and/or thermal expansion coefficient exists between AT particles and glass–ceramic matrix.

4. Conclusions

(1) Glass–ceramics in the diopside system containing 5 and 10 wt.% AT particle show good sintering behavior with desirable final density.

(2) Adding aluminum titanate to the mentioned glass–ceramic matrix up to 10 wt.% can improve its mechanical properties. Young's modulus and thermal expansion coefficient differences between glass–ceramic and AT particles are the main reasons for crack deflection found as a prevalent mechanism responsible for improved bending strength. However the composite containing 20 wt.% AT does not show good property due to incomplete densification and dissolution of diopside phase at its sintering temperature.

References

[1] Z. Strnad, Glass–ceramic Materials, Elsevier Science Publishing Company, New York, 1986.

[2] H.A.J. Thomas, R. Stevens, Aluminium titanate—a literature review, Br. Ceram. Trans. 88 (1989) 144–190.

[3] H. Morishima, Z. Kato, K. Uematsu, K. Saito, Development of aluminum titanate–mullite composite having high thermal shock resistance, J. Am. Ceram. Soc. 69 (10) (1986) 226–227.

[4] D.P.H. Hasselman, K.Y. Donaldson, Effect of thermal history on the thermal diffusivity and thermal expansion of an alumina–aluminum titanate composite, J. Am. Ceram. Soc. 76 (9) (1993) 2180–2184.

[5] N.P. Padture, S.J. Bennison, H.M. Chan, Flaw-tolerance and crack-resistance properties of alumina–aluminum titanate composites with tailored microstructures, J. Am. Ceram. Soc. 76 (9) (1993) 2312–2320.

[6] R. Uribe, C. Baudin, Influence of a dispersion of aluminum titanate particles of controlled size on the thermal shock resistance of alumina, J. Am. Ceram. Soc. 86 (5) (2003) 846–850.

[7] A.R. Boccaccini, K. Pfeiffer, H. Kern, Thermal shock resistant Al_2TiO_5–glass matrix composite, J. Mater. Sci. Lett. 18 (1999) 1907–1909.

[8] P. Alizadeh, M. Yousefi, B. Eftekhari Yekta, N. Ghafoorian, F. Molaie, Sintering behavior of SiO_2–CaO–MgO (Na_2O) glass–ceramics system, Ceram. Int. 33 (2007) 767–771.

[9] P. Alizadeh, B. Eftekhary Yekta, A. Gervei, Effect of Fe_2O_3 addition on the sinterability and machinability of glass–ceramics in the system MgO–CaO–SiO_2–P_2O_5, J. Eur. Ceram. Soc. 24 (2004) 3529–3533.

[10] J.E. Shelby, Introduction to Glass Science and Technology, The Royal Society of Chemistry, Cambridge, 1997, pp. 120–122.

[11] Y. Ohya, Z. Nakagawa, Crack healing and bending strength of aluminum titanate ceramics at high temperature, J. Am. Ceram. Soc. 71 (5) (1988) 232–233.